



UNIVERSITÀ DI PARMA

ARCHIVIO DELLA RICERCA

University of Parma Research Repository

Effect of fillers and their fractional voids on fundamental fracture properties of asphalt mixtures and mastics

This is the peer reviewed version of the following article:

Original

Effect of fillers and their fractional voids on fundamental fracture properties of asphalt mixtures and mastics / Roberto, Antonio; Romeo, Elena; Montepara, Antonio; Roncella, Riccardo. - In: ROAD MATERIALS AND PAVEMENT DESIGN. - ISSN 1468-0629. - 21:1(2020), pp. 25-41. [10.1080/14680629.2018.1475297]

Availability:

This version is available at: 11381/2852377 since: 2020-06-10T09:29:27Z

Publisher:

Taylor and Francis Ltd.

Published

DOI:10.1080/14680629.2018.1475297

Terms of use:

Anyone can freely access the full text of works made available as "Open Access". Works made available

Publisher copyright

note finali coverpage

(Article begins on next page)



Effect of Fillers and their Fractional Voids on Fundamental Fracture Properties of Asphalt Mixtures and Mastics

Journal:	<i>Road Materials and Pavement Design</i>
Manuscript ID	Draft
Manuscript Type:	Original Scientific Paper
Keywords:	HMA mixtures, mineral filler, rigid void, fracture, digital image correlation

SCHOLARONE™
Manuscripts

Effect of Fillers and their Fractional Voids on Fundamental Fracture Properties of Asphalt Mixtures and Mastics

A laboratory investigation was performed to evaluate the influence of filler type and Rigden fractional voids on fundamental fracture limits of asphalt mixtures and mastics. Fracture properties of 14 different asphalt mixtures and mastics composed by the combination of seven different fillers and two asphalt binders, were evaluated using: a visco-elastic fracture mechanics-based crack growth law for mixtures; the Bending Beam Rehometer for mastics at low temperatures and a Modified Direct Tension Test (MDTT) for mastics at intermediate temperatures. A Digital Image Correlation System (DIC) was employed to detect strain distribution and damage evolution in mastics. Experimental results indicate that the filler type and Rigden fractional voids affect the fracture limits and the definition of strain distribution and damage evolution of both mixtures and mastics, while other properties result more dependent on the physio-chemical interaction between filler and asphalt binder.

Keywords: HMA mixtures; mineral filler; rigden void; fracture; digital image correlation

Introduction

It has long been recognized that Hot Mix Asphalt (HMA) mechanical behaviour is strongly related to the properties of the mastic and the interaction between asphalt binder and mineral filler (Anderson and Goetz, 1973; Craus et al., 1976). Filler in asphalt mixture has the role of filling the voids between coarse aggregates and interacts physio-chemically with the asphalt binder, influencing the performance and the workability of asphalt mixture (Delaporte et al, 2008; Faheem and Bahia, 2009; Faheem et al., 2012; Kim et al, 2003; Zhang et al., 2016). As discussed by many authors (Jiménez et al., 2011; Wang et al., 2011; Yi-qiu et al., 2010; Zeng et al., 2008) the stiffness of the mastic affects the ability of the mixture to resist permanent deformation at higher temperatures, influences stress development and fatigue resistance at

1
2
3 intermediate temperatures, and influences stress development and fracture resistance at
4
5 low temperatures. Mineral filler fractional voids value has been used as an indicator of
6
7 filler stiffening effect since the introduction of the test by Rigden in 1947. He
8
9 considered the asphalt required to fill the voids in the dry compacted bed as fixed
10
11 asphalt, while asphalt in excess of that amount was defined as free asphalt, indicating
12
13 that the percent free asphalt is the main factor defining the consistency of the filled
14
15 system. Many studies were later conducted to evaluate the influence of the filler's
16
17 fractional voids on the performance of mastic and mixtures (Kim and Little, 2004,
18
19 Lackner et al., 2005, Little and Petersen 2005). All these studies agree that the stiffness
20
21 of the mastic is higher than that of the binder and that such stiffening effect increases as
22
23 the fractional voids increase. More recently, Faheem et al. (2010 and 2012) performed
24
25 an important study to evaluate the effect of Rigden Void (RV) test values on the
26
27 stiffening effect of fillers as determined by measuring the viscosity of the unfilled
28
29 binders and filled mastics system. They found that the RV can demonstrate the potential
30
31 of stiffening effect of fillers, but showed that, when the same filler is blended with
32
33 different asphalt binders, the measured RVs of the fillers cannot provide sufficient
34
35 guidance on the interaction between the filler and the binder.
36
37
38
39

40
41 Very few studies were conducted to better understand the role of fillers and their
42
43 fractional voids on the cracking behaviour of asphalt mixtures and mastics. To this
44
45 scope, accurate description of strain evolution and distribution in mastics is essential for
46
47 revealing significant information on the binder-filler interaction.
48

49
50 The present study evaluates the influence of mineral fillers and their fractional
51
52 voids on fundamental fracture properties of asphalt mixtures and mastics. The
53
54 objectives of this research were:
55
56
57
58
59
60

- Evaluate how Rigden Void of fillers influences the low temperature properties of mastics.
- Evaluate how Rigden Void of fillers influences the fundamental cracking properties of asphalt mixtures using and appropriate crack growth law.
- Evaluate how the interaction between asphalt binder and filler influences the mastic cracking behavior at intermediate temperatures using appropriate Digital Image Correlation analyses.

Seven different fillers were associated to two asphalt binders (one unmodified and one polymer modified) to obtain 14 asphalt mixtures and mastics. The filler fractional voids were calculated according to the European Norms procedure (EN 1097-4).

The cracking performance of the mixtures at intermediate temperature were evaluated using the visco-elastic fracture mechanics-based cracking model “HMA Fracture Mechanics” (Roque et al. 2002; Zhang et al. 2001). According to this model, only five tensile mixture properties, easily obtainable from the Superpave Indirect Tensile Test (IDT), are required to control the cracking performance of asphalt mixtures. They are the tensile creep rate as represented by the power law creep compliance relationship (m-value), the resilient modulus, the creep compliance, the dissipated creep strain energy to failure ($DCSE_f$) and the total energy to fracture (FE).

The behavior of the mastics at low temperatures was estimated conducting the Superpave Bending Beam Rehometer (BBR) test (AASHTO T 303 2002) over a wide range of low temperatures. The cracking behaviour of the mastics at intermediate temperatures was investigated using a Modified Direct Tension Test (MDTT) developed by Montepara et al. (2011). Strain localization and damage distribution were observed using an in-house developed DIC software code, called DICE, which was

1
2
3 completely re-designed (Dall'Asta et al. 2016) from the first DIC code developed by
4
5 Birgisson et al. (2006 & 2009).
6

7 The results showed that the filler type and Rigden fractional voids values do not
8
9 affect some parameters, which result more dependent on other properties (i.e. resilient
10
11 modulus and creep compliance of mixtures and stiffness of mastic at low temperatures).
12
13 Conversely, fundamental fracture limits of both asphalt mixtures and mastics, and the
14
15 definition of strain distribution and damage evolution during damage, result affected by
16
17 both the filler nature and Rigden Voids.
18
19

20 21 22 **Experimental Methods** 23

24 The influence of the Rigden Voids on mixture's cracking behavior was evaluated at low
25
26 temperatures for mastics, and at intermediate temperatures for both asphalt mixtures and
27
28 mastics. The Bending Beam Rheometer (BBR) test was performed to determine the
29
30 stiffness and m-value of mastics at low temperatures (-30°C, -24°C, -18°C, -12°C and -
31
32 6°C). The cracking properties of asphalt mixtures at intermediate temperature were
33
34 evaluated applying a fundamental failure mechanism entitled HMA Fracture
35
36 Mechanics, proposed by Zhang et al. (2001) and Roque et al. (2002). The cracking
37
38 behaviour of the mastics was investigated using a Modified Direct Tension Test
39
40 (MDTT) developed on purpose, to identify crack initiation and interpret mastic fracture
41
42 response at intermediate temperature (Montepara et al. 2011). Strain localization and
43
44 damage distribution were observed using a new Digital Image Correlation System
45
46 (DIC) developed at the University of Parma (Dall'Asta et al. 2016), obtaining 2D full-
47
48 field strain maps of both mastics and HMA specimens during tensile loading.
49
50
51
52
53

54 55 ***Bending Beam Rheometer (BBR) Test*** 56

57 BBR test was conducted to investigate the effect of the different fillers on mastics at
58
59
60

1
2
3 low temperatures. The mastic beams (125 mm long, 12.5 mm wide and 6.25 mm thick)
4
5 were submerged in a constant temperature bath and kept at test temperature for 60 min.
6
7 A constant weight of 100 g was then applied to the mastic beam, which was supported
8
9 at both ends, and the deflection of center point was measured continuously. Creep
10
11 stiffness (S) and creep rate (m) were measured at several loading times ranging from 8
12
13 to 240 s.
14
15

16 17 *Asphalt Mixture Cracking Properties*

18
19 According to the HMA Fracture Mechanics framework, failure of asphalt mixtures is
20
21 governed by two fundamental properties: Fracture Energy density threshold (FE) and
22
23 Dissipated Creep Strain Energy threshold ($DCSE_f$). These two properties are easily
24
25 obtainable from three mechanical mixture tests performed at 10°C in an indirect tension
26
27 test configuration: resilient modulus (Roque and Buttlar 1992), creep compliance
28
29 (Buttlar and Roque 2004) and tensile strength (Roque et al. 1997). The FE limit is
30
31 determined as the area under the stress-strain curve, while the $DCSE_f$ is the fracture
32
33 energy minus the elastic energy at the time of fracture.
34
35

36
37 The $DCSE_f$ is a measure of how much micro-damage mixture can take before it
38
39 results in a macrocrack initiation. In order to predict top-down cracking performance of
40
41 the mixture in the field, an Energy Ratio criterion was proposed by Roque et al. (2004).
42
43 The Energy Ratio is defined as follows:
44
45

$$46 \quad ER = \frac{DCSE_f}{DCSE_{min}} \quad (1)$$

47
48 where $DCSE_f$ is the dissipated creep strain energy threshold of the mixture and $DCSE_{min}$
49
50 is the minimum dissipated creep strain energy required, a function of the creep
51
52 compliance power law parameters. Basically, $DCSE_{min}$ is a measure of how much
53
54
55
56
57
58
59
60

1
2
3 damage will the material accumulate in the field during service life. For a good field
4 performance of the mixture $ER > 1$ is required.
5
6
7

8 *Mastic Fracture Test*

9
10
11 The cracking behavior of the mastics was investigated using a Modified Direct Tension
12 Test (MDTT) developed on purpose, to identify crack initiation and interpret mastic
13 fracture response at intermediate temperature. The test was developed modifying the
14 Standard SuperPave™ DTT test for asphalt binders. All the details can be found
15 elsewhere (Montepara et al. 2011).
16
17
18
19
20
21

22
23 MDTT tests were performed on three replicates at 15°C using an MTS closed-
24 loop servo-hydraulic loading system adopting a 2.5kN load cell. The specimen was
25 fixed at one end and pulled from the other end applying a constant stroke of 1.68
26 mm/sec until rupture occurs. The engineering stress was computed according to the
27 SuperPave™ binder specification:
28
29
30
31
32

$$33 \sigma_f = \frac{P_f}{A_0} \quad (2)$$

34
35
36
37
38
39 where: σ_f = failure stress; P_f = measured load at failure; A_0 = original cross-sectional
40 area.
41
42

43
44 Failure is defined as the point on the stress-strain curve where the load reaches its
45 maximum. The rapid loading rate and the interpretation of the test only up to fracture
46 allow for a continuum representation. Strains were obtained from DIC system,
47
48 interpolating all the strain values of the grid points located at the 46x20 mm specimen
49 central cross-sectional area. The test configuration is shown in Figure 1.
50
51
52
53
54
55
56
57
58
59
60

Mastic Strain Analysis

Mastic strains during loading were obtained using an in-house developed DIC software, code called DICE, which implements an innovative Least Squares Matching approach that uses higher order polynomial shape functions to model the displacement field between the reference and the measured image of the DIC sequence, proposed also by other authors in different application fields (Bethmann and Luhmann, 2010). The DIC system has shown to achieve satisfactory accuracy compared to strain gauges, resulting in 0.04% accuracy in compressive/tensile strains and 0.03% accuracy in shear strains (Dall'Asta et al 2016).

A digital camera Basler piA1600-35gm (resolution 1608x1308, focal length 8mm, pixel size 7.4 micrometers, 35 fps@max resolution), directly connected to the testing control system, is located on a support inside the climatic chamber where tests are performed. The chamber is provided with a proper LED lighting system which assures good illumination without heating up the specimen. Since the crack phenomenon is very fast and short-lasting (1÷2 seconds), the camera was properly set up to acquire the images in a smaller area of the sensor (300x500 pixel) reducing the bandwidth required for transmitting each frame and, consequently, allowing a higher frame rate (ca. 80 fps). Thanks to the elongated shape of the specimen, once provided an optimal imaging geometry, the reduced size of the images still allowed the complete acquisition of the whole specimen surface. The images are automatically processed by the software, providing accurate displacement/strain fields. To achieve high accuracies in the strain field measurements, the specimen surface must present a well-contrasted grey scale speckle pattern, easily obtainable by a water paint-based treatment (Romeo 2013).

Materials

Fourteen asphalt mixtures and fourteen respective mastics were used in this study. All the mixtures were 12.5-mm nominal maximum size, produced with limestone, marly limestone and calcarenite and composed by the same aggregate type and gradation (Figure 2). Two different asphalt binders were used in this research: N is an unmodified binder graded as PG 58-22 while M is a SBS polymer modified binder graded as PG64-22 (3.5% of SBS linear polymers).

Fillers

Seven fillers were associated to the two binders: a limestone (not pure) filler labeled as B; a limestone filler containing high percentages of magnesium carbonate, labeled as D; a filler obtained from the grinding of coal rocks, labeled as R; a fly ash filler, labeled as FA; a pure limestone filler labeled as L; the combination of pure limestone filler and 20% of hydrated lime, labeled as HL and a stabilized fly ash, labeled as S obtained from Municipal Solid Waste Incinerator (MSWI). The method to inert fly ash from MSWI with a low temperature process has been developed and patented by Bontempi et al. (2010a and 2010b) and Zacco et al. (2012), within a project supported by LIFE program of the European Community (LIFE + 2008 project ENV/IT/000434).

Following are the properties of four materials:

- Filler “B” (not pure limestone) is composed of CaCO_3 (90%), $\text{CaMg}(\text{CO}_3)_2$ (6%) and SiO_2 (4%) with a density of 2.73 g/cm^3 and a Rigden Void of 37.0%
- Filler “D” is composed of CaCO_3 (60%) and MgCO_3 (40%), with a density of 2.84 g/cm^3 and a Rigden Void of 38.21%

- Filler “R” (not pure limestone) is composed of CaCO_3 (>80 %), Cl^- (<0.004 %), S (<0.002 %) and H_2O (<0.5 %) with a density of 2.71 g/cm^3 and a Rigden Void of 36.30%.
- Fly ash “FA” filler is composed of SiO_2 , Al_2O_3 , Fe_2O_3 , CaO , with a density of 2.37 g/cm^3 and a Rigden Void of 37.30%.
- Filler “L” is pure limestone composed of CaCO_3 (100%), with a density of 2.71 g/cm^3 and a Rigden Void of 40.16%.
- Filler “HL” composed of CaCO_3 (80%), and $\text{Ca}(\text{OH})_2$ (20%) with a density of 2.64 g/cm^3 and a Rigden Void of 44.5%.
- Filler “S” is mainly composed of calcite, hannebachite ($2\text{CaSO}_3 \cdot \text{H}_2\text{O}$), crystalline and amorphous silicon oxide phases and soluble salts (sodium chloride, NaCl and potassium chloride, KCl) with a density of 2.57 g/cm^3 and a Rigden Void of 64.66%.

Fractional voids were calculated for the fillers according to the European Norms procedure (EN 1097-4) rather than the National Asphalt Pavement Association (NAPA) version, due to larger sample used and availability of equipment. A detailed description of mastics and asphalt mixtures is given in Table 1.

HMA Specimen preparation

Two aggregate batches of 4500 g of aggregates were prepared for each mixture to produce a total of 56-152 mm diameter cylindrical specimens. The batches were mixed (at 160°C for unmodified mixes and 170°C for modified mixes) with the design asphalt content percentage (5.2%) and heated for two hours at 135°C for short-term aging. The cylindrical specimens were obtained compacting the mixes to $6 (\pm 0.5)$ percent air voids into 152 mm diameter specimens using the Pine Gyrotory Compactor. Each cylindrical

specimen was sawn to obtain two effective plates, each 30 mm thick discarding the top and the bottom plates for reducing density gradient effects. For each mixture, four circular shaped specimens were used to perform resilient modulus, creep compliance, and strength test at 10° C according to the Superpave IDT procedure developed by Roque and Buttlar (1992) and Buttlar and Roque (1994).

Mastic Specimen preparation

The mastic specimens were prepared following the improved SuperPave™ binder testing specimen preparation procedure suggested by Ho and Zanzotto (2000). The selected filler concentration was 60% by weight for all mastic formulations in order to maintain the same filler/mastic content as the asphalt mixtures.

For each specimen, 28 g of asphalt binder and 42 g of filler were prepared and heated at mixing temperature (160°C for unmodified binders and 170°C for modified ones) in separate tins for 30 minutes. Then, the filler was slowly added to the asphalt in the oven. A mechanical mixer, with a maximum nominal angular speed of 8,000 rpm, was used to blend the materials at mixing temperatures. The mixing process was carefully followed so that the filler was homogeneously dispersed in the binder. The mastic was continuously stirred as it cooled to prevent settling and then was poured to the preheated dog-bone shaped aluminum mold. The specimen is allowed to cool to room temperature for one hour and de-molded. It is then placed in the environmental control chamber for one hour at testing temperature before the test is performed.

Results and analysis

Rigden Voids and Low Temperature Properties of Mastics

BBR test was conducted at -30, -24, -18°C, -12 and -6°C for all blends in five

1
2
3 replicates. Results of BBR low temperature stiffness at a loading time of 60 s, are
4
5 shown in Figures 3 and 4 for unmodified and modified asphalt binder, respectively;
6
7 while m-values are indicated in Table 2.
8

9
10 Generally, increasing stiffness means that the thermal stresses developed in the
11
12 pavement due to low temperature also increase, and thermal cracking become more
13
14 likely. On the other hand, decreasing m-value indicates declining the rate of stress
15
16 relaxation, which also increases the probability of thermal cracking.
17

18
19 The results clearly show that mastic stiffness and m-value are not directly
20
21 influenced by the Rigden Voids of fillers, but rather that both binder and filler type
22
23 affect low temperature properties of mastics. The unmodified mastics generally exhibit
24
25 higher stiffness than the modified ones. Filler B produces a very high stiffness when
26
27 combined with the neat binder but exhibits the lowest stiffness when combined with the
28
29 modified binder. Similarly FA, when combined with the neat binder, produces a high
30
31 stiffness but not when combined with the modified binders. This indicates that binder
32
33 modification mitigates the stiffening effect of some fillers at low temperatures. Finally,
34
35 fillers HL and S exhibit lower m-values combined with both neat and modified binders,
36
37 indicating low rate of stress relaxation.
38
39

40
41 In conclusion, Rigden Void of fillers does not govern low temperature properties
42
43 of the mastics, which are mainly influenced by the interaction between binder and filler.
44
45

46 47 ***Rigden Voids and Cracking Properties of Mixtures***

48
49 A summary of Superpave IDT test results and a detailed analysis of each mixture
50
51 property is presented. All the tests were performed on three replicates at 10°C using an
52
53 MTS closed-loop servo-hydraulic loading system. The relationship between filler
54
55 Rigden Voids and mixture cracking performance is also described. All the results
56
57
58
59
60

1
2
3 obtained from the Superpave IDT test are listed in Table 3.
4
5

6 7 *Resilient Modulus*

8
9 The resilient modulus is a measure of the material's elastic stiffness since it corresponds
10 to the ratio of the applied stress to the recoverable strain with repeated loading. The
11 results listed in Table 3 show that Rigden Voids and filler nature, have no significant
12 effect on resilient modulus. The very low difference among the all values indicates that
13 the elastic response at small strain and/or short loading is mainly governed by the
14 aggregate skeleton, rather than by the interaction between asphalt binder and their single
15 properties.
16
17
18
19
20
21
22
23
24

25 26 *Creep Compliance*

27
28 Creep compliance represents the time-dependent behaviour of asphalt mixture, thus it is
29 commonly used to evaluate the rate of damage accumulation. The crack growth process
30 is exhibited by higher rates of permanent deformation, thus mixtures with high creep
31 rates show higher crack growth rates. Creep compliance curves are shown in Figures 5
32 and 6 for unmodified and modified mixtures, respectively. The curve trends are very
33 similar regardless of the type of filler employed. The only presence of filler S (stabilized
34 fly ash from MSWI) increases significantly the rate of permanent deformation leading
35 to higher rate of micro-damage accumulation. This is likely due to the particular
36 composition of the filler which chemically interacts with the asphalt binder causing
37 significant permanent deformation. Conversely, the introduction of hydrated lime
38 decreases the creep compliance for both unmodified and modified binders. The most
39 important role is played by the type of binder; indeed modified mixtures show creep
40 compliance significantly lower than those obtained with unmodified binders.
41
42
43
44
45
46
47
48
49
50
51
52
53
54
55
56
57
58
59
60

1
2
3 In summary, the results highlight that the creep compliance of mixtures is not
4 affected by the Rigden Void of fillers, but rather by the type of asphalt binder and the
5 particular interaction between binder and filler in the mastic.
6
7
8

9 10 11 *Energy-Based Parameters*

12
13 Energy-based parameters are easily determined from the stress-strain response of a
14 tensile strength test, as discussed by Roque et al. (2002). Fracture Energy (FE) density
15 is the energy per unit volume required to fracture a mixture and it is determined as the
16 area under the stress-strain curve at first fracture, while Dissipated Creep Strain Energy
17 (DCSE) at failure is defined as the fracture energy minus the elastic energy at the time
18 of fracture.
19
20
21
22
23
24
25
26

27 Results listed in Table 3 show that tensile strengths generally increase with the
28 increase of Rigden Voids, while tensile strains at failure exhibit the opposite trend.
29 More interestingly, as shown in Figure 7, mixtures containing fillers with Rigden Voids
30 higher than 4% show an increase of more than 50% in both Fracture Energies and
31 Dissipated Creep Strain Energies with respect to those mixtures containing fillers with
32 Rigden Voids lower than 4%. This is true for both unmodified and polymer modified
33 mixtures. Energy Ratio parameters, which govern the trend of the mixture to resist to
34 top-down cracking, are clearly more dependent to the type of asphalt binder employed.
35
36
37
38
39
40
41
42
43
44
45

46 *Mastic Fracture Behaviour*

47
48 From MDTT test, fracture energies were computed as the area under the stress-strain
49 curve at the point of failure, which is defined as the point on the curve where the load
50 reaches its maximum. The rapid loading rate and the interpretation of the test only up to
51 fracture allow for a continuum representation. Strains were obtained from DICe,
52 interpolating all the strain values of the grid points located at the 46x20 mm specimen
53
54
55
56
57
58
59
60

1
2
3 central cross-sectional area.
4

5 Tensile strengths, strains at failure and fracture energies are listed in Table 4.
6
7 The results confirm what previously observed from IDT tests: mastics composed by
8
9 filler with Rigden Voids higher than 4% show higher fracture energies, for both
10
11 unmodified and modified binders (Figure 8). According to the test results, fillers have
12
13 shown to play an important role in defining failure parameters: mastics containing filler
14
15 S (stabilized flay ash from MSWI) show high tensile strengths and low deformability
16
17 exhibiting a brittle behavior; mastics composed by filler L (pure limestone) show good
18
19 tensile resistance and high deformability, which are both increased by the addition of
20
21 hydrated lime (filler HL). The remaining mastics exhibit lower fracture energies; some
22
23 of them make the mastic more brittle with high tensile resistance and small strains to
24
25 failure (filler C), others increase ultimate strain showing lower resistance to failure
26
27 (filler R). This is true for both unmodified and polymer modified mixtures. Figure 9
28
29 show full-field tensile (ϵ_{yy}) strain maps at crack initiation for 4 mastics, obtained from
30
31 the combination of unmodified asphalt binder and the 4 fillers that better describe the 4
32
33 more typical behavior. Same trends were obtained with mastics composed by polymer
34
35 modified asphalt binder. Filler S allows mastics to localize strains in a small area
36
37 corresponding to the localization of impending fracture, where exhibits high strain
38
39 concentration, resulting in a brittle behavior whit high fracture limits. Filler HL allows
40
41 the strains to distribute more in a restricted area, leading to high failure limits together
42
43 with a significant deformability. Filler C makes the mastic more brittle leading to a
44
45 fracture point at low values of failure strains which are, at the same time, highly
46
47 distributed. Finally, filler R causes highly distributed damage in a large area leading to
48
49 high deformability but low tensile strength resistance.
50
51
52
53
54
55
56
57
58
59
60

Summary and Conclusion

The influence of mineral fillers and their fractional voids on asphalt mixture and mastics fundamental cracking failure limits were investigated. Fourteen asphalt mixtures and mastics composed by the combination of two asphalts (one unmodified and one SBS polymer modified) and seven different fillers were examined. According to the HMA Fracture Mechanics visco-elastic cracking model, the following findings on mixtures cracking behaviour were obtained:

- The type of filler and Rigden Voids do not affect Resilient Modulus of mixtures indicating that the elastic response at small strain and/or short loading is mainly governed by the aggregate skeleton, rather than by the interaction between asphalt binder and fillers and their single properties.
- The type of filler and Rigden Voids generally do not affect creep-related performance. Conversely, the rate of damage accumulation mainly depends on the asphalt binder nature. The only filler S increases significantly the rate of permanent deformation due to the particular composition of the filler, which probably causes an important chemical reaction that should be investigated further.
- Energy based parameters (fracture energy and dissipated creep strain energy) have shown to be affected by the filler nature and Rigden Voids. In detail, mixtures containing fillers with Rigden Voids higher than 4% show significantly higher energy limits (more than 50%). Conversely, tensile strengths have shown to not depend directly on the filler nature but rather on the interaction between filler and asphalt binder. Finally the Energy Ratio, governing the mixture resistance to top-down cracking is more dependent to the type of asphalt binder employed.

1
2
3 Stiffening effect of fillers at low temperatures were investigated performing the
4 BBR on mastics. It was observed that filler nature and Rigden Voids do not govern low
5 temperature properties of the mastics, which are mainly influenced by the interaction
6 between binder and filler.
7
8
9
10

11 Mastic fracture behavior was examined performing the MDTT test associated
12 with the Digital Image Correlation software DICe. According to the test results, mastics
13 composed by filler with Rigden Voids higher than 4% show higher fracture energies,
14 for both unmodified and modified binders, as obtained from mixtures. Moreover, fillers
15 have shown to play an important role in defining failure parameters, especially in
16 defining strain distribution and evolution during damage, showing the own capability of
17 releasing deformability to the mastic.
18
19
20
21
22
23
24
25
26
27

28 **References**

- 29
30
31 AASHTO T 303 (2002). Standard test method for determining the flexural creep
32 stiffness of asphalt binder using the Bending Beam Rheometer (BBR), T 313-02,
33 American Association of State Highway and Transportation Officials,
34 AASHTO, Washington DC.
35
36
37 Anderson D.A., Goetz W.H. (1973) "Mechanical Behavior and Reinforcement of
38 Mineral Filler-Asphalt Mixtures". *Journal of the Association of Asphalt Paving*
39 *Technologists*, 42, pp. 37-66.
40
41
42 Bethmann F., Luhmann T. (2010) "Least-squares matching with advanced geometric
43 transformation models". *International Archives of Photogrammetry, Remote*
44 *Sensing and Spatial Information Sciences*, XXXVIII (5), pp. 86-91.
45
46
47 Birgisson B., A. Montepara, Napier J.A.L., Romeo E., Roncella R., Tebaldi G. (2006).
48 "Micromechanical Analyses for Measurement and Prediction of HMA Fracture Energy"
49 *Journal of the Transportation Research Record*, 1970, pp: 186-195.
50
51
52 Birgisson B., Montepara A., Romeo E., Roque R., Roncella R., Tebaldi G. (2009) "An
53 Optical Strain Measurement System for Asphalt Mixtures". *Materials and*
54 *Structures*, 42, pp. 427-441.
55
56
57
58
59
60

- 1
2
3 Bontempi E., Zacco A., Borgese L., Gianoncelli A., Ardesi R., Deper, L.E. (2010a). “A
4 new powder filler, obtained by applying a new technology for fly ash
5 inertization procedure”. *Advances in Science and Technology*, 62, pp. 27–33.
6
7
8 Bontempi E., Zacco A., Borgese L., Gianoncelli A., Ardesi R., Depero L.E. (2010b). “A
9 new method for Municipal solid waste incinerator (MSWI) fly ash inertization,
10 based on colloidal silica”. *Journal of Environmental Monitoring*, 12, pp. 2093–
11 2099.
12
13
14 Buttlar W.G. and Roque R., (1994). “Development and Evaluation of the Strategic
15 Highway Research Program Measurement and Analysis System for Indirect
16 Tensile Testing at Low Temperatures”. *Transportation Research Record*, 1454,
17 pp. 163-171.
18
19
20
21 Craus J., Ishai I., Sides A. (1976) “Some Physiochemical Aspects of the Effect and Role
22 of the Filler in Bituminous Paving Mixtures”. *Journal of The Association of
23 Asphalt Paving Technologists*, 45, pp. 558-588.
24
25
26 Dall’Asta E., Ghizzardi V., Brighenti R., Romeo E., Roncella R., Spagnoli A. (2016).
27 “New experimental techniques for fracture testing of highly deformable
28 materials”. *Frattura ed Integrita Strutturale*, 10(35), pp. 161-171.
29
30
31 Delaporte B., Di Benedetto H., Chaverot P., Gauthier G. (2008). “Effect of Ultrafine
32 Particles on Linear Viscoelastic Properties of Mastics and Asphalt Concretes”
33 *Transportation Research Record*, 2051, pp. 41–48.
34
35
36 European Committee for Standardization EN 1097-4 (1999) Tests for Mechanical and
37 Physical Properties of Aggregates, Part 4, Determination of the Voids of Dry
38 Compacted Filler. Brussels: CEN.
39
40
41 Faheem A.F. and Bahia U. H. (2009) “Conceptual Phenomenological Model for
42 Interaction of Asphalt Binders with Mineral Fillers” *Journal of the Association
43 of Asphalt Paving Technologists*, 78, pp. 680–717.
44
45
46 Faheem A.F. and Bahia H.U. (2010) “Modeling of Asphalt Mastic in Terms of Filler-
47 Bitumen Interaction”. *Road Materials and Pavement Design*, 11(1), pp. 281-303
48
49
50 Faheem A.F., Hintz C., Bahia U.H., Al-Qadi I., Glidden S., (2012) “Influence of Filler
51 Fractional Voids on Mastic and Mixture Performance”. *Transportation Research
52 Record*, 2294.
53
54
55 Ho S.M.S, Zanzotto L. (2000) “Sample Preparation for Direct Tension Testing –
56 Improving Determination of Asphalt Binder Failure Stress and Test
57 Repeatability”. *Transportation Research Record*, 1766, pp. 15-23.
58
59
60

- 1
2
3 Jiménez F.P., Recasens R.M., Martínez A. (2011) “Effect of filler nature and content on the
4 behavior of bituminous mastics”. *Road Materials and Pavement Design*, doi:
5 10.1080/14680629.2008.9690177
6
- 7 Kim Y.K., Little D.L., Song I. (2003) “Effect of Mineral Fillers on Fatigue Resistance
8 and Fundamental Material Characteristics: Mechanistic Evaluation”.
9 *Transportation Research Record*, 1832, pp. 1-8.
10
- 11 Kim Y.R. and Little D.N. (2004) “Linear Viscoelastic Analysis of Asphalt Mastics”.
12 *Journal of Materials in Civil Engineering*, 16(2), pp. 122-132.
13
- 14 Lackner R, Spiegl M, Blab R, Eberhardsteiner J (2005) “Is Low-Temperature Creep of
15 Asphalt Mastic Independent of Filler Shape and Mineralogy? Arguments from
16 Multiscale Analysis”. *Journal of Materials in Engineering*, 17(5), pp. 485-491.
17
- 18 Little D. and Petersen J.C. (2005) “Unique Effects of Hydrated Lime Filler on the
19 Performance Related Properties of Asphalt Cements: Physical and Chemical
20 Interactions Revisited”. *Journal of Materials in Civil Engineering*, 17(2), pp.
21 207-218.
22
- 23 Montepara A., Romeo E., Isola M., Tebaldi G. (2011). “The role of fillers on cracking
24 behavior of mastics and asphalt mixtures”. *Journal of the Association of Asphalt
25 Pavement Technologists*, 80, pp. 161–191.
26
- 27 Ridgen PJ (1947) “The Use of Fillers in Bituminous Road Surfacing – A Study of
28 Filler-Binder System in Relation to Filler Characteristics”. *Journal of Society of
29 Chemical Industry*, 66, pp. 9-299.
30
- 31 Romeo E. (2013) “Two-dimensional digital image correlation for asphalt mixture
32 characterisation: interest and limitations” *Road Materials and Pavement Design*, 14(4),
33 pp. 747-763
34
- 35 Roque R. and Buttlar W.G. (1992) “The Development of a Measurement and Analysis
36 System to Accurately Determine Asphalt Concrete Properties Using the Indirect
37 Tensile Mode”. *Journal of the Association of Asphalt Paving Technologists*, 61,
38 pp. 304-332.
39
- 40 Roque R., Birgisson B., Sangpetgnam, B., Zhang, Z. (2002). “Hot Mix Asphalt Fracture
41 Mechanics: A Fundamental Crack Growth Law for Asphalt Mixtures”. *Journal
42 of the Association of Asphalt Paving Technologist*, 71, pp. 816-827.
43
- 44 Roque R., Birgisson B., Drakos C., Dietrich B. (2004). “Development and Field
45 Evaluation of Energy-Based Criteria for Top-down Cracking Performance of
46
47
48
49
50
51
52
53
54
55
56
57
58
59
60

- 1
2
3 Hot Mix Asphalt”. *Journal of the Association of Asphalt Paving Technologists*,
4 73, pp. 229-260.
- 5
6 Zacco A., Gianoncelli R., Ardesi S., Sacrato L., Guerini E., Bontempi E., Tomasoni M.,
7 Alberti L., Depero E. (2012). “Use of colloidal silica to obtain a new inert from
8 municipal solid waste incinerator (MSWI) fly ash: First results about reuse”.
9 *Clean Technologies and Environmental Policy*, 14(2), pp. 291–297.
- 10
11 Zeng M. and Wu C. (2008). “Effects of type and content of mineral filler on viscosity of
12 asphalt mastic and mixing and compaction temperatures of asphalt mixture”,
13 *Transportation Research Record*, 2051, pp. 31-40.
- 14
15 Zhang Z., Roque R., Birgisson B., Sangpetgnam B. (2001). “Identification and
16 Verification of a Suitable Crack Growth Law”. *Journal of the Association of
17 Asphalt Paving Technologists*, 70, pp. 206-241
- 18
19 Zhang J., Liu G., Zhu C., Pei J. (2016) “Evaluation indices of asphalt–filler interaction
20 ability and the filler critical volume fraction based on the complex modulus”.
21 *Road Materials and Pavement Design*, doi:10.1080/14680629.2016.1218789
- 22
23 Yi-qiu T., Li Z.H., Zhang X.Y., Dong, Z.J. (2010). “Research on high- and low-
24 temperature properties of asphalt-mineral filler mastic”, *Journal of Materials in
25 Civil Engineering*, 22(8), pp. 811-819.
- 26
27 Wang H., Al-Qadi I.L., Faheem A.F., Bahia H.U., Yang S.H. and Reinke G.H. (2011).
28 “Effect of mineral filler characteristics on asphalt mastic and mixture rutting
29 potential”. *Transportation Research Record*, 2208, pp. 33-39.
- 30
31
32
33
34
35
36
37
38
39
40
41
42
43
44
45
46
47
48
49
50
51
52
53
54
55
56
57
58
59
60

Table 1. Mastic/Asphalt Mixture definition

Mastic/Mixture Label	Binder	Filler
NB	Natural - PG58-22	Limestone (not pure)
ND	Natural - PG58-22	Limestone + Magnesium carbonate
NR	Natural - PG58-22	Coal rocks
NFA	Natural - PG58-22	Fly ash
NL	Natural - PG64-28	Limestone (pure)
NHL	Natural - PG64-28	Limestone + Hydrated Lime (20%)
NS	Natural - PG64-28	Inertized MSWI fly ash
MB	SBS Modified - PG64-22	Limestone (not pure)
MD	SBS Modified - PG64-22	Limestone + Magnesium carbonate
MR	SBS Modified - PG64-22	Coal rocks
MFA	SBS Modified - PG64-22	Fly ash
ML	SBS Modified - PG64-22	Limestone (pure)
MHL	SBS Modified - PG70-22	Limestone + Hydrated Lime (20%)
MS	SBS Modified - PG70-22	Inertized MSWI fly ash

Table 2. BBR m-values of mastics

Temp [°C]	m-value (@60 s)				
	-30	-24	-18	-12	-6
NB	0.129	0.175	0.279	0.419	0.606
ND	0.128	0.211	0.296	0.429	0.612
NR	0.144	0.162	0.274	0.397	0.579
NFA	0.133	0.185	0.296	0.391	0.573
NL	0.113	0.165	0.253	0.404	0.545
NHL	0.120	0.167	0.208	0.356	0.539
NS	0.120	0.161	0.209	0.330	0.497
MB	0.181	0.211	0.294	0.426	0.547
MD	0.163	0.200	0.291	0.416	0.533
MR	0.154	0.190	0.291	0.432	0.558
MFA	0.173	0.185	0.276	0.403	0.563
ML	0.137	0.200	0.288	0.424	0.516
MHL	0.142	0.183	0.258	0.357	0.509
MS	0.114	0.183	0.209	0.361	0.501

Table 3. Superpave IDT results

Asphalt Mixture	Resilient Modulus [GPa]	Creep Compliance [1/GPa]	Tensile Strength [Mpa]	Faliure strain (μ strain)	Fracture Energy [kJ/m^3]	DCSE _r [kJ/m^3]	DCSE _{min} [kJ/m^3]
NB	18.32	2.45	1.71	1.224	1.43	1.345	1.399
ND	17.22	2.18	2.26	0.917	1.36	1.213	1.269
NR	17.36	2.14	1.60	1.335	1.38	1.307	1.164
NFA	18.31	2.37	2.08	1.078	1.44	1.326	1.336
NL	17.25	2.23	2.49	1.350	1.68	1.500	1.430
NHL	16.35	1.98	2.12	1.690	2.15	2.011	1.292
NS	16.80	3.72	2.65	1.010	1.98	1.771	1.847
MB	18.86	0.74	1.69	0.904	1.07	0.990	0.379
MD	19.14	0.99	1.30	1.549	1.74	1.705	0.335
MR	17.04	0.83	2.13	0.838	1.30	1.165	0.439
MFA	17.89	1.04	1.32	1.453	1.29	1.235	0.531
ML	16.30	1.12	2.56	1.750	2.86	2.658	0.877
MHL	15.32	0.82	2.45	1.965	2.99	2.788	0.866
MS	17.50	2.85	3.01	1.468	2.58	2.116	1.132

Table 4. Mastic MDTT results

Asphalt Mixture	Tensile Strength [Mpa]	Faliure strain (μ strain)	Fracture Energy [kJ/m^3]
NB	0.46	9.18	4.35
ND	0.41	12.75	4.29
NR	0.33	17.32	4.87
NFA	0.50	7.73	4.12
NL	0.52	15.62	5.12
NHL	0.58	16.32	6.30
NS	0.73	11.24	6.22
MB	0.43	12.34	3.12
MD	0.57	10.32	4.98
MR	0.40	13.23	3.98
MFA	0.63	7.43	4.01
ML	0.75	13.87	8.32
MHL	0.83	14.30	9.35
MS	0.76	12.12	8.12

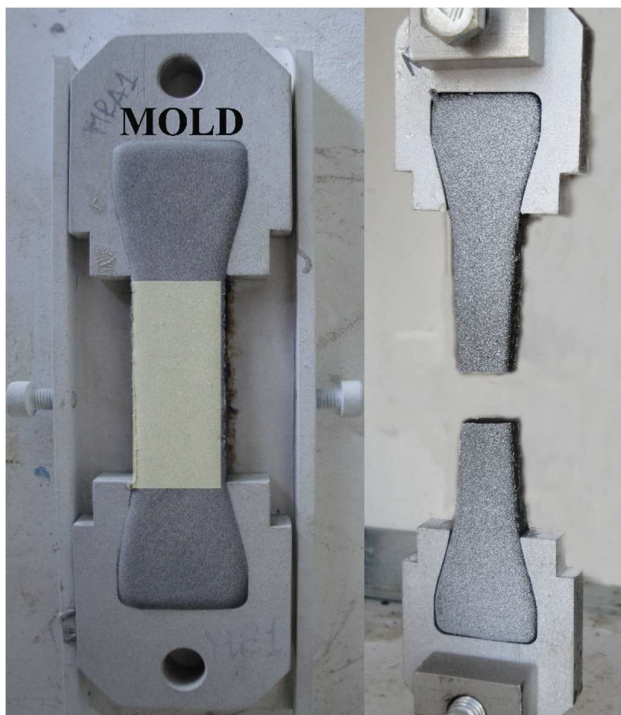


Figure 1. MDDT test configuration (on the left the area of interest for DIC)

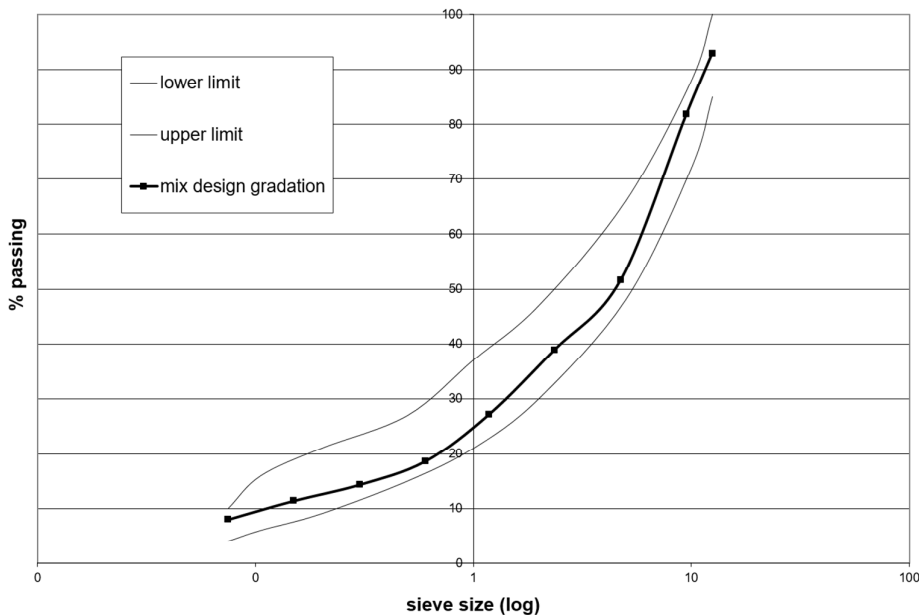


Figure 2. Aggregate gradation of the mixtures

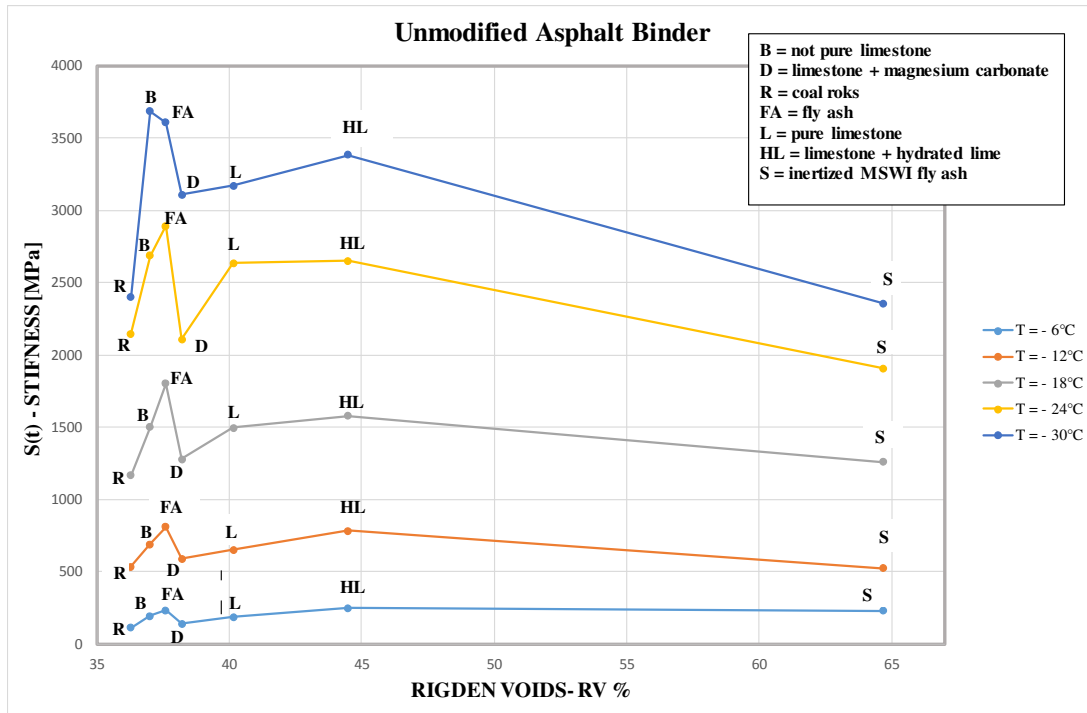


Figure 3. Stiffness of unmodified asphalt mastics according to Rigden Voids

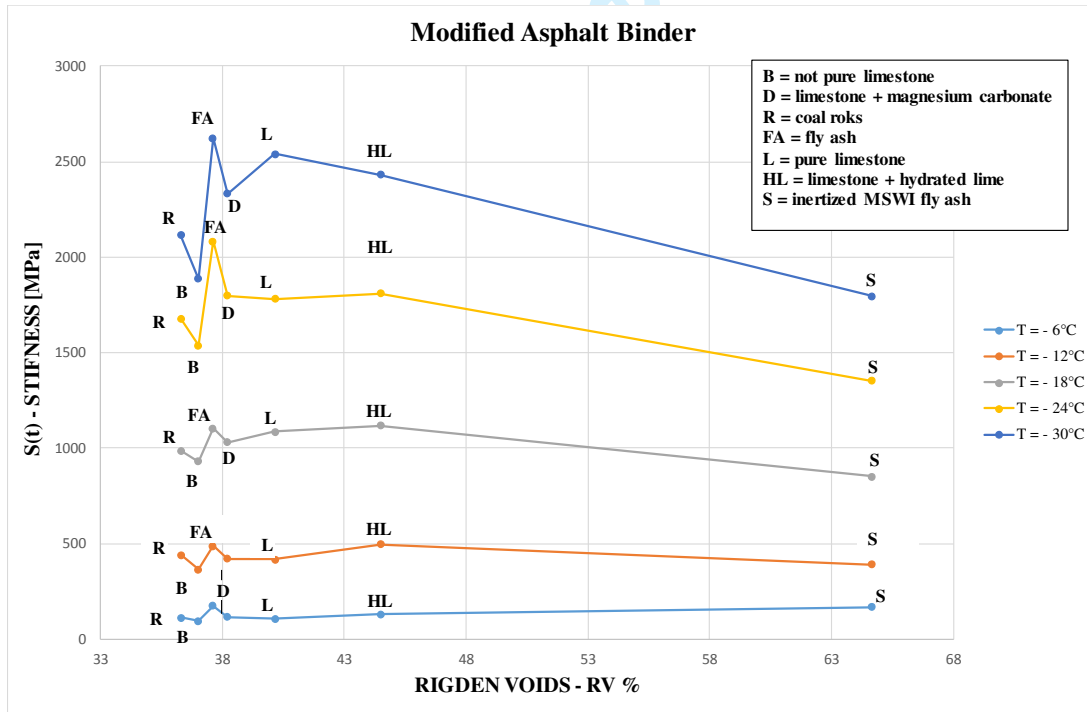


Figure 4. Stiffness of modified asphalt mastics according to Rigden Voids

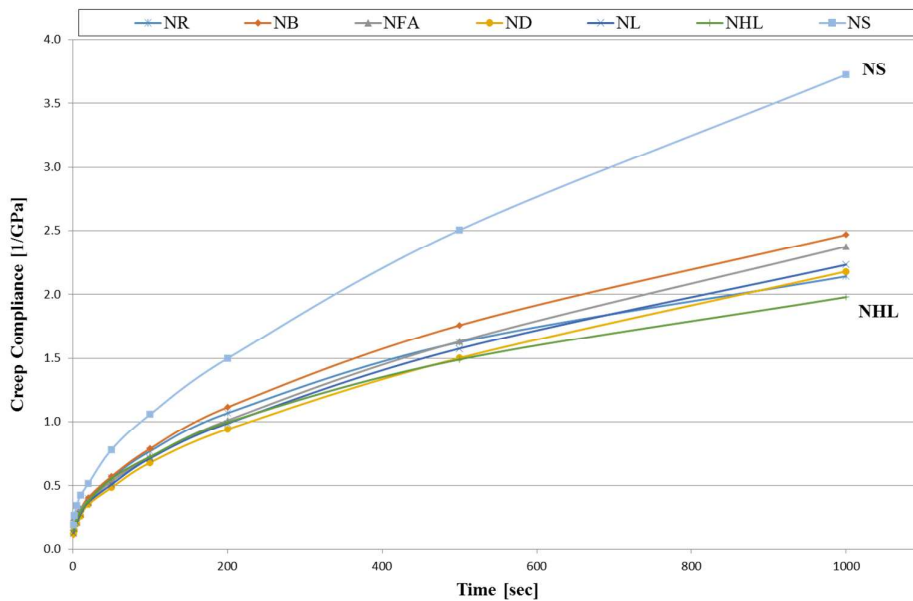


Figure 5. Creep Compliance Curves for unmodified mixtures

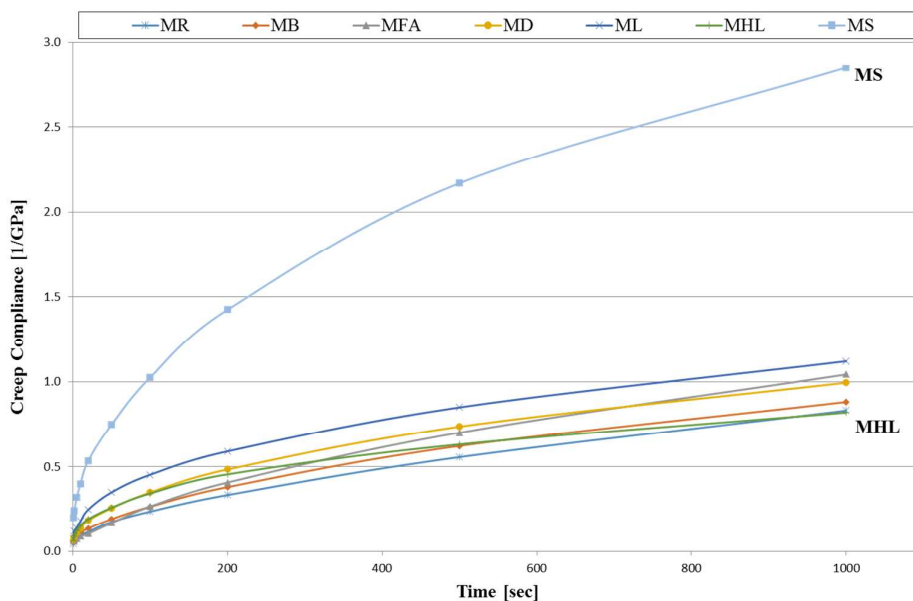


Figure 6. Creep Compliance Curves for modified mixtures

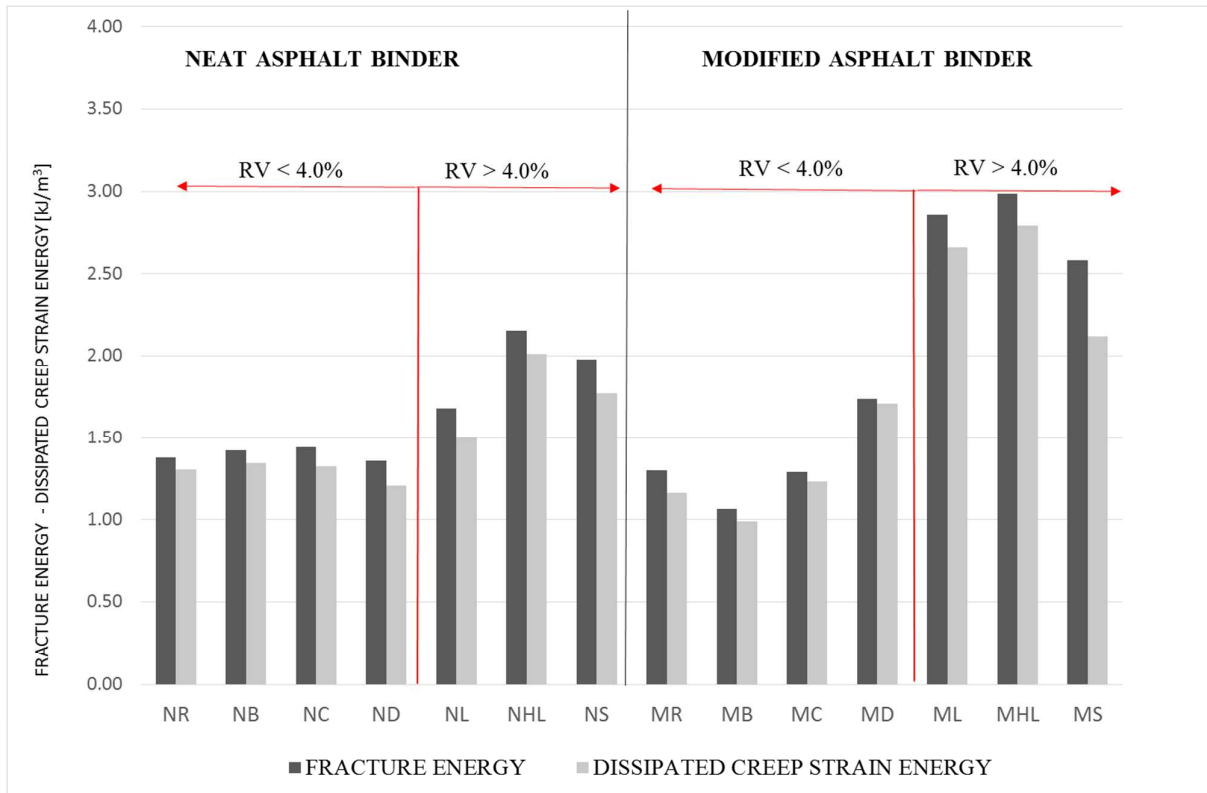


Figure 7. Fracture Energy and Dissipated Creep Strain Energy of mixes in function of Rigden Voids

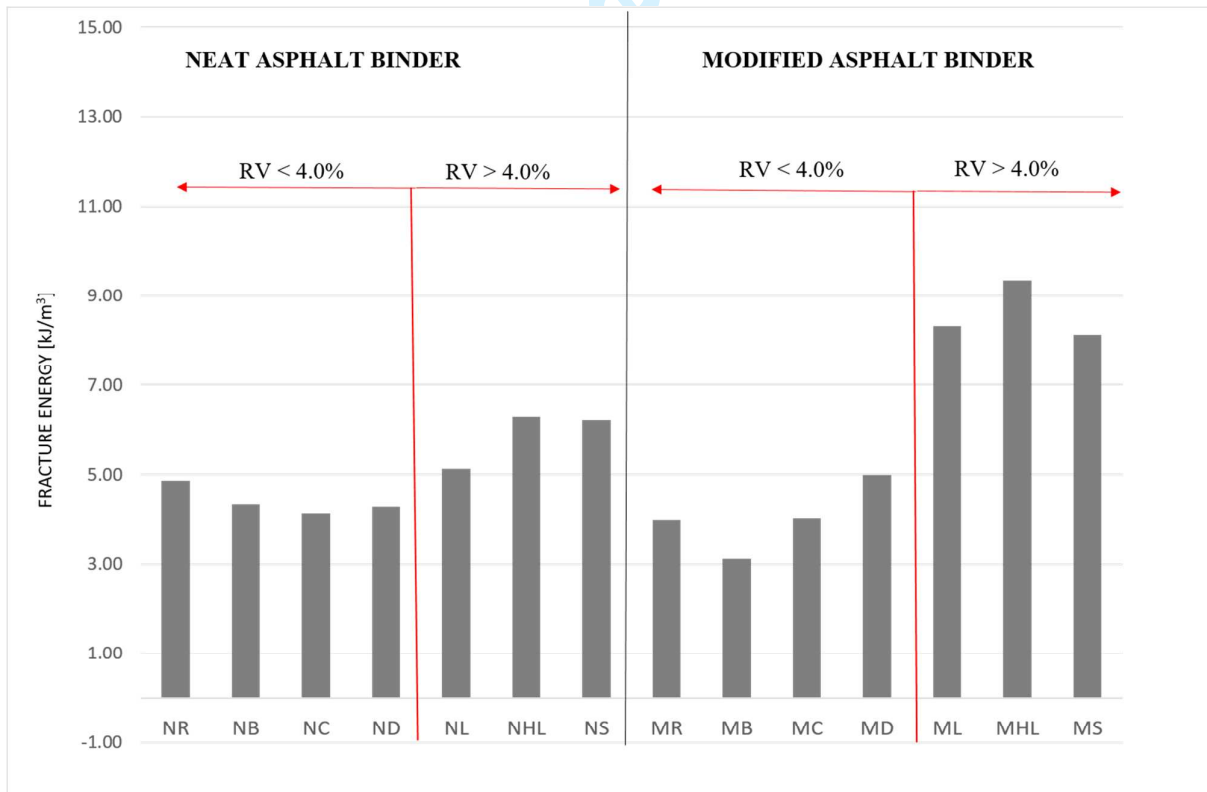


Figure 8. Fracture Energy of mastics in function of Rigden Voids

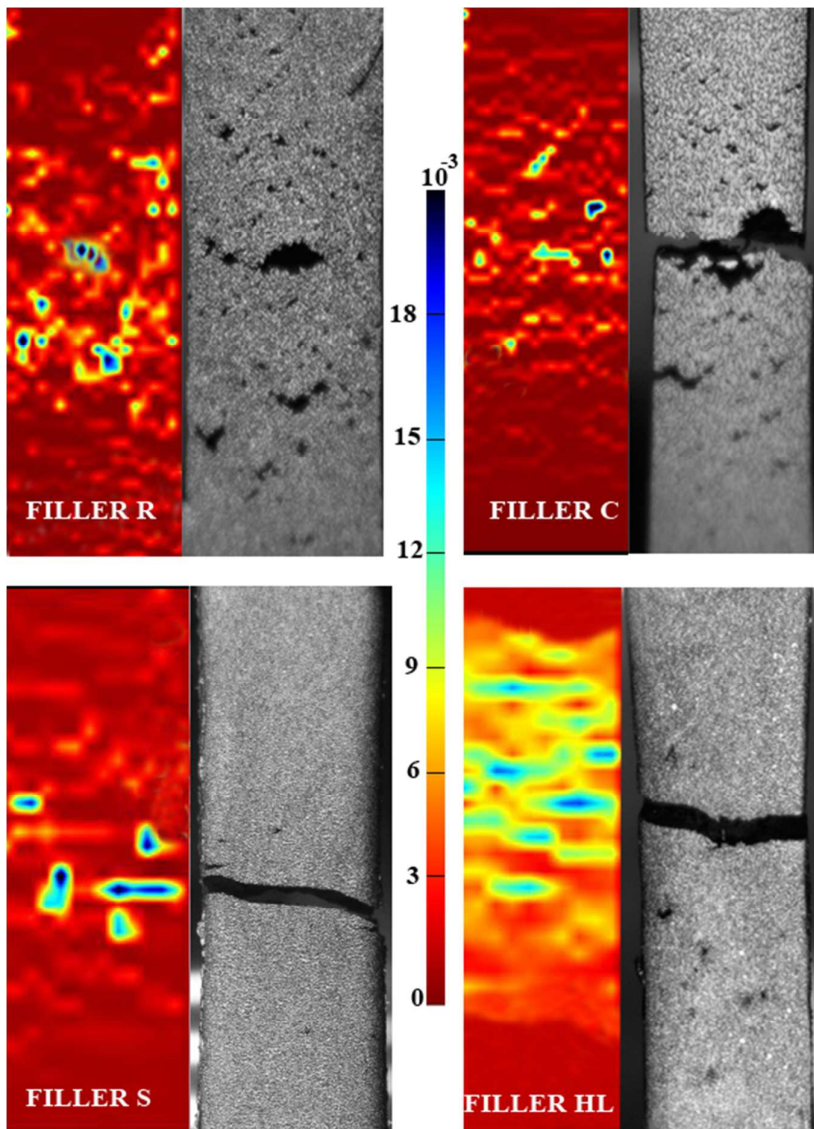


Figure 9. Crack patterns of mastics containing more critical fillers and unmodified binder